

**An Exception to Carnot's Theorem Inferred from Tolman's Experiment: Ion-Containing Fluids Driving Continuous Heat-to-Electricity Conversion under Acceleration (A Stable and Sustainable Environmental Energy Source for Continuous Thermal-to-Electric Energy Conversion Utilizing the Effect of Acceleration Forces Causing Internal Voltage Gradients)**

Kuo Tso Chen

OPTROMAX Co. Taiwan, Zhudong Township, Hsinchu County 310658, Taiwan (R.O.C.)

**CORRESPONDING AUTHOR**

E-mail: gtchen0@gmail.com.

Phone: +886-918-629-588

## **ABSTRACT**

The second law of thermodynamics is widely regarded as unbreakable, with past attempts to refute it failing under scrutiny. In 2015, the author hypothesized that gravity could impart a directional component to molecular motion, potentially converting thermal energy into electrical energy without requiring a temperature difference. This hypothesis, which was extended to plasmas and electrolytes with ions of differing masses by 2022, was experimentally confirmed later that year. Tolman reported a similar electromotive force (EMF) in electrolytes under centrifugal and gravitational fields in 1910, although no prior research connected his findings to thermodynamics. Our study revisits this overlooked phenomenon, demonstrating how ionic solutions under a gravitational or centrifugal field generate a significant potential difference due to mass-dependent ion behavior, and how this potential difference differs from that of metals. Ionic solutions produce measurable and sustained EMFs, which can drive a current when connected in a conductive loop. We theoretically and experimentally validate that the current remains continuous, as any deviation from equilibrium during electron exchange creates a driving force that re-establishes the potential difference. After electrons release electrical energy externally along the forward electromotive force, the resulting internal electron vacancies must be compensated by electron movement driven by the internal counter electromotive force. As thermal vibrations promote the diffusion of ions toward equilibrium, they also facilitate the counter-directional movement of electrons. This counter electromotive motion enables electrons to regain electrical energy internally through thermal vibrational energy, thereby achieving stable and sustained thermal-to-electrical energy conversion. Thus, this mechanism of converting thermal energy into electrical energy surpasses the constraints of Carnot's theorem, providing a solution to Maxwell's demon problem proposed by Maxwell 154 years ago. As a concrete example, we show that using hydrogen iodide (HI) under specified conditions can theoretically

produce approximately 72 W per cubic meter of electrolyte and material, highlighting its potential as a stable and emission-free energy source. These findings reinforce Tolman's results and provide a novel thermodynamic framework for energy conversion.

**Keywords:** Second Law of Thermodynamics; Carnot's Theorem; Tolman Experiment; Electrolyte; Ion-Containing Fluid; Centrifugal Force; Gravitational Field; Energy Conversion; Boltzmann Distribution; Maxwell's Demon

## 1. Introduction

In today's energy landscape, addressing global warming and finding effective energy conversion methods are critical challenges. Many energy systems rely on converting thermal energy into mechanical or electrical energy. However, according to Carnot's theorem, for heat engines operating with two baths, the maximum efficiency of the work output-to-heat input ratio is the temperature difference between the two baths divided by the absolute temperature, which means that once heat is transferred from a high-temperature region to a low-temperature region and loses its temperature gradient, the thermal energy can no longer be converted into usable energy.

The second law of thermodynamics<sup>2</sup> is considered an unbreakable iron law<sup>2</sup>. Historically, any claims of violating this law have been proven incorrect<sup>2</sup>. However, in 1910, Tolman reported that electrolytes subjected to centrifugal and gravitational forces generate electric fields, with different electrolytes exhibiting varying field magnitudes<sup>3</sup>. If two separate tubular containers filled with different electrolytes are placed in the same gravitational field and electrically connected at the bottom, a voltage difference will develop at the top. When moving from the higher potential side to the lower potential side, electrons in the upper region inevitably result in energy release. If the upper ends are also electrically connected, a spontaneous circulating current will emerge, enabling continuous electrical energy output. On the basis of the principle of energy conservation, the spontaneous energy output must have a corresponding energy source. In a system where only electron exchange occurs without any other material exchange and where each region maintains electrical neutrality, gravity cannot perform work on the system. Consequently, thermal energy remains the only possible source for the output energy. Furthermore, this energy conversion can take place even when all regions have the same temperature. Thus, this mechanism of converting thermal energy into electrical energy surpasses

the constraints of Carnot's theorem, providing a solution to Maxwell's demon problem<sup>4</sup> proposed by Maxwell 154 years ago. Tolman believed that this potential difference was caused by polarization, meaning that charge accumulation would eventually stop the current. However, our experiments, conducted at a site where the daily temperature fluctuation was less than 1.5°C and no air conditioning airflow was present, show that the current remains stable and continuous without weakening due to charge accumulation. To ensure experimental rigor and eliminate electromagnetic interference, the sample was kept stationary inside an iron cabinet throughout the long-duration current output experiments. This finding indicates that the thermal vibrational energy of molecules and ions is sufficient to overcome the polarization effect that Tolman proposed and continuously regenerates the potential difference. Consequently, this thermal vibrational energy becomes the most likely source of energy, and we will later explain how electricity drives charged particles to move against the electric field and thereby gain electrical energy—thus exceeding the limitations of Carnot's theorem.

We have been contemplating possible exceptions to the second law of thermodynamics for a long time. In 2015, we realized that gravity could impart directionality to molecular motion rather than allowing completely random movement, potentially providing an opportunity to surpass the second law of thermodynamics, which is based on chaotic motion. In September 2021, we realized that in plasmas, the force exerted by an electric field on ions is proportional to their charge, whereas the force exerted by gravity is proportional to their mass. Since these two forces do not follow the same proportionality, different plasmas generate different potential differences. In April 2022, we noticed that ions in electrolytes exhibited similar effects, and later that year, we experimentally confirmed this phenomenon by measuring results identical to those obtained by Tolman in 1910<sup>3</sup>. Furthermore, we verified that this voltage difference can persist for extended periods while maintaining the external energy output.

However, it is intriguing why, for over a century, no one identified Tolman's conclusions as a means to surpass the limitations of the second law of thermodynamics.

In the following text, we use the Boltzmann distribution<sup>5</sup> to deduce why gravity can generate an internal electric field within an ion-containing fluid rather than merely producing an external electric field at the fluid's surface. Additionally, we employ an approach analogous to Maxwell's reasoning<sup>4</sup> to explain how two parallel fluid systems composed of different ions can spontaneously generate an electric current even in the absence of a temperature difference, and we theoretically estimate the average amount of electrical energy released per electron exchange.

Through theoretical derivation, we found that when the pH of an electrolyte is close to 7, even a small difference in ion concentration can cause significant changes in pH and chemical potential. In contrast, when the pH deviates significantly from 7, the same change in ion concentration results in only small changes in pH and chemical potential. This characteristic leads to a nonlinear relationship between the gravitational force (or centrifugal force) and the resulting voltage difference when the pH is near 7. This insight provides an explanation for the observed nonlinear behavior in the experimental results, highlighting the sensitivity of the system under near-neutral pH conditions.

Additionally, theoretically, under specific conditions derived from our theoretical framework, an aqueous solution of hydrogen iodide (HI) can generate approximately 72 W of electrical energy per cubic meter of structural material and electrolyte.

Consider a rotating system: if the rotation speed is doubled, the centrifugal force increases fourfold, meaning that only a quarter of the original distance is required to generate the same voltage difference. By connecting four such systems in series, the total voltage difference could reach four times the original value. Given that the resistance of the conductor is proportional to its thickness under the same cross-sectional area, the resistance at a quarter of the

original distance would be one-fourth of the original value. Thus, the energy output from each system would be four times greater. If four systems are placed in the same space, it can be inferred that such a design could significantly increase the energy output efficiency by up to 16 times, whereas the air resistance energy consumption would only increase by approximately four times. Therefore, increasing the rotational speed could lead to the generation of practically usable electrical energy. In addition, there are many other ways to increase the output power, some of which are mentioned in the text.

In conclusion, thermal vibrational energy drives charged particles to overcome both electric fields and gravitational or centrifugal forces. Through motion induced by the counter-electromotive force, these particles acquire electrical energy, replenishing regions where energy has been depleted due to voltage differences or conductive interface-driven energy output. Since the system can sustain energy exchange under accelerating conditions, even in the absence of a temperature gradient and without rotational inertia losses, this process could surpass the limitations of Carnot's theorem, offering a mechanism for continuously converting ambient thermal energy into usable electrical energy.

## **2. Qualitative Explanation of the Causes of Spontaneous Electric Fields within Plasma in a Gravitational Field**

The higher concentration of gases at the Earth's surface than at high altitudes is due to gravitational effects. Under the same height difference, the concentration gradient for lighter gas molecules is relatively small, whereas for heavy gas molecules, the concentration gradient is more significant—an observation widely acknowledged. Consider Figures 1(a) and 1(b). In Figure 1(a), yellow circles represent lighter gas molecules, whereas in Figure 1(b), blue circles represent heavier gas molecules. When both gases have equal molecular quantities and each

region maintains the same temperature and average pressures, heavier molecules will be more concentrated in the lower region along the direction of gravity, whereas lighter molecules will be more concentrated in the upper region, opposite to the gravitational direction. When these gases are mixed under isothermal and isobaric conditions, as illustrated in Figure 1(c), gas kinetic theory dictates that, in the absence of any chemical reactions and with only physical collisions occurring, the height-dependent distribution of molecules does not change significantly. Now, replacing lighter gas molecules with negatively charged ions of equal mass and heavier gas molecules with positively charged ions of equal mass, as shown in Figure 1(d), the overall system remains electrically neutral because of the equal number of ions. However, since heavier ions are more concentrated in the lower region and lighter ions are more concentrated in the upper region, the lower region acquires a net positive charge in the absence of ion movement, whereas the upper region acquires a net negative charge. This results in the formation of an electric field directed from bottom to top. This electric field drives ion migration, causing heavier positive ions to move upward, whereas lighter negative ions move downward. As ions move, the net charge in both the upper and lower regions decreases, weakening the electric field. Ion movement continues until the combined force of the electric field and gravitational pull acting on each ion type reaches equilibrium. At this point, the ions maintain a stable concentration gradient—intermediate between those depicted in Figure 1(d). Additionally, the central region remains nearly electrically neutral, leading to a cessation of net ion movement. At equilibrium, a small residual electric field remains to sustain the concentration gradient of lighter ions above what would be expected in a noncharged system, whereas the concentration gradient of heavier ions remains lower than that in an uncharged state. Consequently, the uppermost region retains a small net negative charge, whereas the lower region retains a small net positive charge, as illustrated in Figure 1(e).

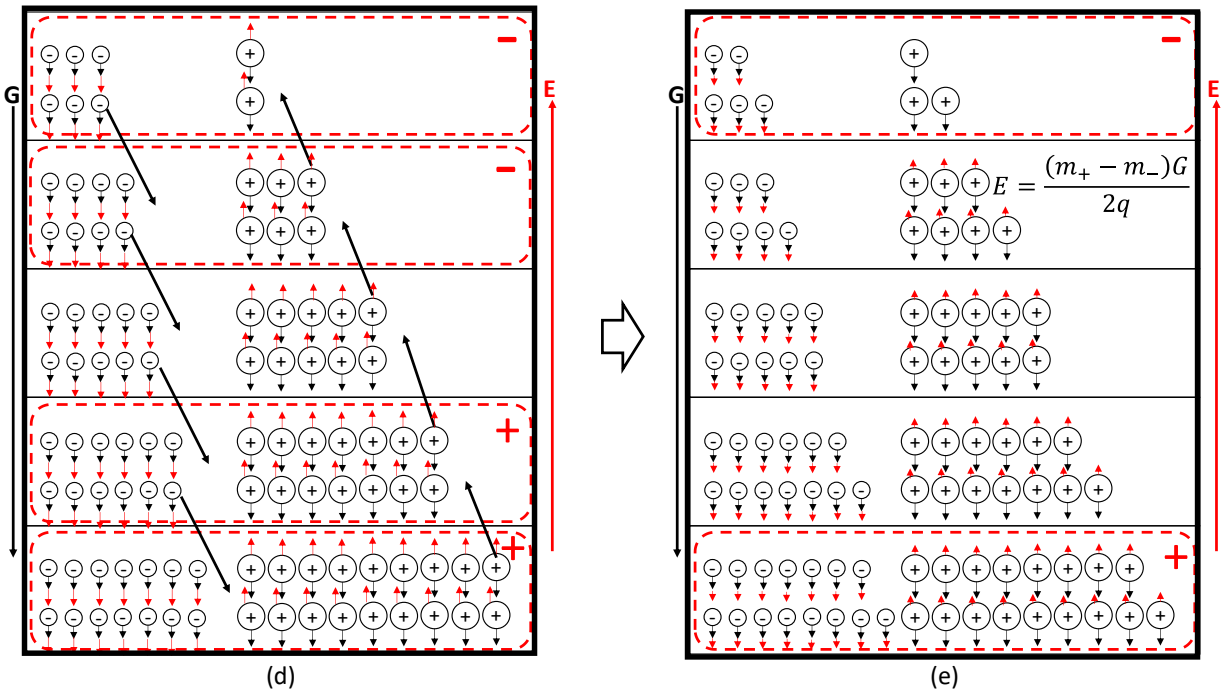
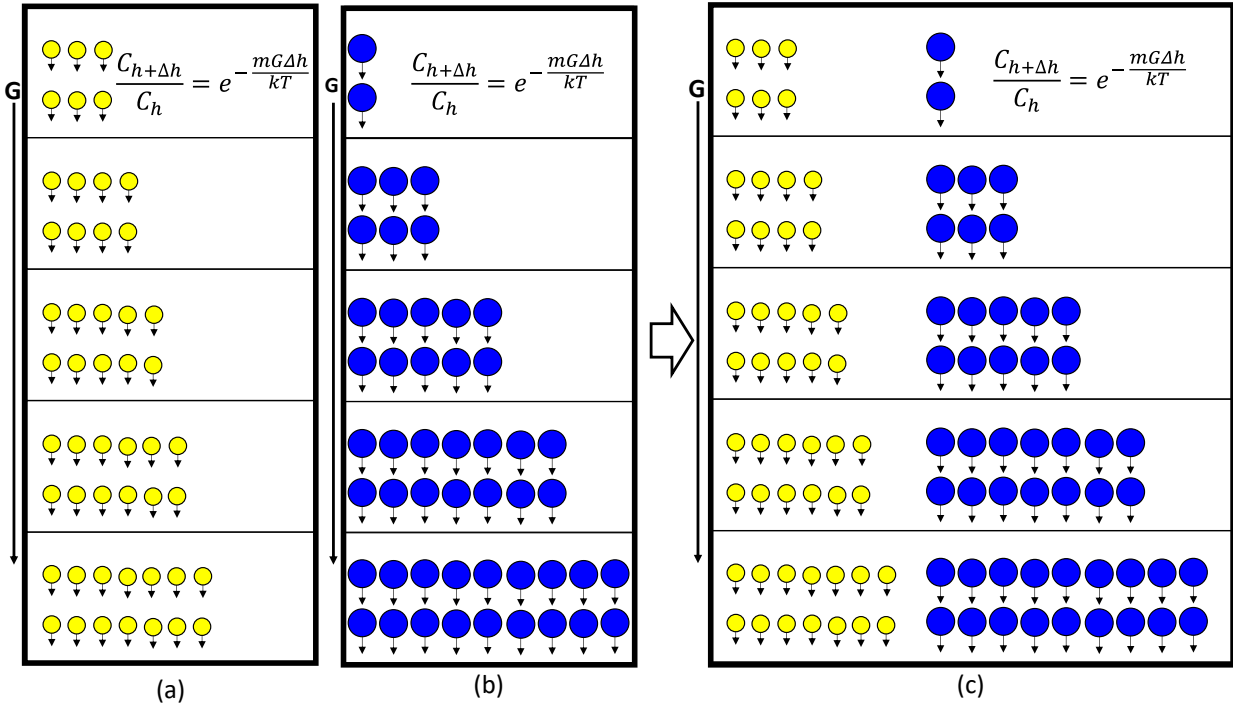


**Fig. 1.** (a) Schematic diagram of the variation in the concentration of light neutral gas molecules with height. (b) Schematic diagram of the variation in the concentration of heavy neutral gas molecules with height. (c) Schematic diagram of the concentration distributions of both light and heavy molecules with height. (d) Schematic diagram of the concentration distributions of both light and heavy molecules with height, showing the forces acting on the ions. (e) Schematic diagram of the concentration distributions of both light and heavy molecules with height, showing the electric field  $E = \frac{(m_+ - m_-)G}{2q}$ .

heavy neutral gas molecules with height when mixed. (d) Schematic diagram of the distribution of light negatively charged ions and heavy positively charged ions in a plasma with height, assuming no electric field or chemical interactions. (e) Schematic diagram of the redistribution of ions in a plasma due to the internally generated electric field, showing the height-dependent variation in light negatively charged ions and heavy positively charged ions, assuming no electrochemical interactions.

### 3. Calculation of Electric Field Strength Generated Within an Ion-Containing Fluid Under an Accelerating Force Field

Specifically, the variation in the concentration of a pure gas with height, when in equilibrium, follows the Boltzmann distribution.<sup>5</sup> The relationship is described by Equation (1).

$$\frac{C_{h+\Delta h}}{C_h} = e^{-\frac{\varepsilon_{h+\Delta h} - \varepsilon_h}{kT}} = e^{-\frac{mG\Delta h}{kT}} \dots \dots \dots \quad (1)$$

where  $h$  is the height coordinate value,  $C_h$  is the concentration of ions at height  $h$ ,  $C_{h+\Delta h}$  is the concentration of ions at height  $h + \Delta h$ ,  $\varepsilon_h$  is the potential energy of the ion at height  $h$ ,  $\varepsilon_{h+\Delta h}$  is the potential energy of the ion at height  $h + \Delta h$ ,  $m$  is the mass of the particle (or ion),  $G$  is gravity,  $mG$  is the gravitational force on the particle (or ion), and  $kT$  is the product of the Boltzmann constant  $k = 1.380649 \times 10^{-23} \text{ J/K}^{11}$  and the thermodynamic temperature  $T$ .

Notably, Equation (1) contains a mass variable  $m$ , meaning that heavier particles will experience a greater change in concentration with height than lighter particles. Thus, in the absence of an electric field, ions with larger masses are subjected to greater gravitational forces, resulting in a larger concentration difference between high and low positions. In contrast, in the absence of an electric field, ions with smaller masses experience weaker gravitational forces, leading to a smaller concentration difference. Therefore, as seen from Equation (1), in the

absence of an electric field and when the masses of positive and negative ions in the plasma are different, the lower region will have a greater number of heavier ions than lighter ions, whereas the upper region will have a greater number of lighter ions than heavier ions. For example, in  $Li^+$  and  $Cl^-$  plasmas, the mass of  $Cl^-$  is approximately 5 times greater than that of  $Li^+$ , so the gravitational force of  $Cl^-$  is also approximately 5 times greater than that of  $Li^+$ . When the number of positive and negative ions is the same, on the basis of equation (1) and the abovementioned principles, in the absence of an electric field, the number of chloride ions  $Cl^-$  will be greater than the number of lithium ions  $Li^+$  in the lower region of the plasma, resulting in a negative charge. In the upper region, the number of chloride ions  $Cl^-$  is less than that of lithium ions  $Li^+$ , resulting in a positive charge. When the electricity above the plasma is positive and the electricity below it is negative, a top-down electric field is generated. This electric field causes  $Cl^-$  to move upward and  $Li^+$  to move downward, reducing the difference in charge between the upper and lower parts. The rates of change of positive ions and negative ions in the plasma with height are the same on the basis of charge balance. That is, when charge balance is achieved, apart from the uppermost and lowermost regions, the intermediate area remains electrically neutral. In the case of charge balance, when the residual electric field strength is  $E$ , equation (2) can be obtained by adding the electric field term  $E$  to the Boltzmann distribution<sup>5</sup> in equation (1), and equation (3) can be derived from equation (2):

$$\frac{C_{Li^+(h+\Delta h)}}{C_{Li^+(h)}} = e^{-\frac{(m_{Li^+}G + qE)\Delta h}{kT}} = \frac{C_{Cl^-(h+\Delta h)}}{C_{Cl^-(h)}} = e^{-\frac{(m_{Cl^-}G - qE)\Delta h}{kT}} \quad \dots \dots \dots \quad (2)$$

$$m_{Li^+}G + qE = m_{Cl^-}G - qE$$

$$E = \frac{(m_{Cl^-} - m_{Li^+})G}{2q} \quad \dots \dots \dots \quad (3)$$

where  $C_{Li^+(h)}$  is the concentration of  $Li^+$  at height  $h$ ,  $C_{Li^+(h+\Delta h)}$  is the concentration of  $Li^+$ s at height  $h + \Delta h$ ,  $m_{Li^+}$  is the mass of  $Li^+$ ,  $E$  is the electric field inside the plasma and is positive in the downward direction,  $G$  is gravity and is positive in the downward direction,  $C_{Cl^-(h)}$  is the concentration of  $Cl^-$  at height  $h$ ,  $C_{Cl^-(h+\Delta h)}$  is the concentration of  $Cl^-$ s at height  $h + \Delta h$ ,  $m_{Cl^-}$  is the mass of  $Cl^-$ , and  $q$  represents the charge of the negative electron, which is  $1.602176634 \times 10^{-19}C$ .

Importantly, the electric field in equation (3) exists within the plasma body. This means that charge accumulation occurs at the upper and lower surfaces and that there is no charge accumulation inside the plasma; however, an electric field is distributed throughout the entire plasma body rather than being confined to its surface. In other words, gravity or a centrifugal force generates an electric field within the conductor (plasma).

Equation (3) provides an explanation for the results of Tolman's 1910 experiment<sup>3</sup>, which demonstrated that increasing the concentration of iodide ions in the same centrifugal field had a minimal effect on the generated voltage. This aligns with our derived Equation (3), which indicates that the electric field within plasmas or conductors depends solely on the individual masses of the ions and is independent of the ion concentration.

From Equation (3), when the height difference is  $H$ , the relationship between the voltage difference and gravity is given by Equation (4). Furthermore, Equation (4) indicates that in the same accelerating force field, the voltage difference varies depending on the ion mass.

$$\nabla V = \frac{(m_{Cl^-} - m_{Li^+})GH}{2q} \quad \dots \dots \dots \quad (4)$$

#### **4. A Hypothetical Process Similar to Maxwell's Demon for Understanding the Phenomenon of Gravity-Induced Thermoelectric Conversion**

As shown in Figure 2-(a), there are two plasma regions: one containing potassium ions and the other containing lithium ions. According to Equations (3) and (4), the positively charged particles are now lithium ions and potassium ions, whereas the negatively charged particles are electrons. When the two plasmas remain independent without exchanging ions or electrons, in equilibrium, the heavier potassium ions experience a stronger gravitational force and thus concentrate more at the lower end. In contrast, the lighter lithium ions, which are subject to weaker gravitational forces, exhibit negligible downward sedimentation tendencies, which, relative to potassium plasma, can initially be disregarded. Additionally, electrons, driven by thermal vibrations, diffuse upward more readily than positive ions do. As a result, in the lower region of the potassium plasma, where the concentration of positive ions is higher, a slight positive charge develops, whereas in the upper region, where the proportion of negative ions is greater, a negative charge forms. This phenomenon is less pronounced in lithium plasma.

If identical apertures are drilled at the upper and lower ends of the partition separating the two plasma regions, allowing only electrons to pass while blocking positive ions, as shown in Figure 2-(b), an imbalance will spontaneously arise. At the upper aperture, the potassium plasma, which has a negative charge, increases the probability of electron transport toward the lithium plasma because of the negative charge influence. Conversely, electrons moving from the lithium plasma toward the aperture experience repulsion from the negative charge, making them more likely to be deflected back into the lithium plasma. As a result, more electrons flow from the potassium plasma to the lithium plasma than in the reverse direction. At the lower aperture, a similar principle applies but in the opposite direction: electrons from the potassium plasma experience an attractive force due to the positive charge, leading to fewer electrons passing into the lithium plasma compared with the reverse flow.

This creates an imbalance: at the upper end, the electron concentration in the potassium plasma decreases, deviating from equilibrium, whereas the electron concentration in the lithium plasma increases, also deviating from equilibrium. Conversely, at the lower end, the electron concentration in the potassium plasma increases, whereas that in the lithium plasma decreases. Both plasmas are also out of equilibrium at the lower end. Driven by the energy of thermal vibrations, particles diffuse and flow toward equilibrium. This diffusion phenomenon generates an upward net electron flow in the potassium plasma and a downward net electron flow in the lithium plasma. In the structure shown in Figure 2-(b), these flows form a counterclockwise electron loop, corresponding to a clockwise electric current. This process resembles Maxwell's hypothetical demon.

It is worth noting that at this stage, in a potassium-ion plasma, the net electron movement driven by thermal vibrations flows from positively charged regions toward negatively charged ones—opposite to the attractive force of positive charges and also opposite to the repulsive force of negative charges on electrons. In other words, the electrons move in the direction counter to the electric field, thereby gaining electric potential energy. Since the driving energy originates from thermal vibrations, this process effectively converts thermal energy into electrical energy. This mechanism is the key to thermal-to-electrical energy conversion.

Therefore, in such a structure, as long as thermal vibrations and gravity coexist, a net electron flow is generated. This electron flow can be utilized to convert thermal energy into electrical energy without a temperature gradient.

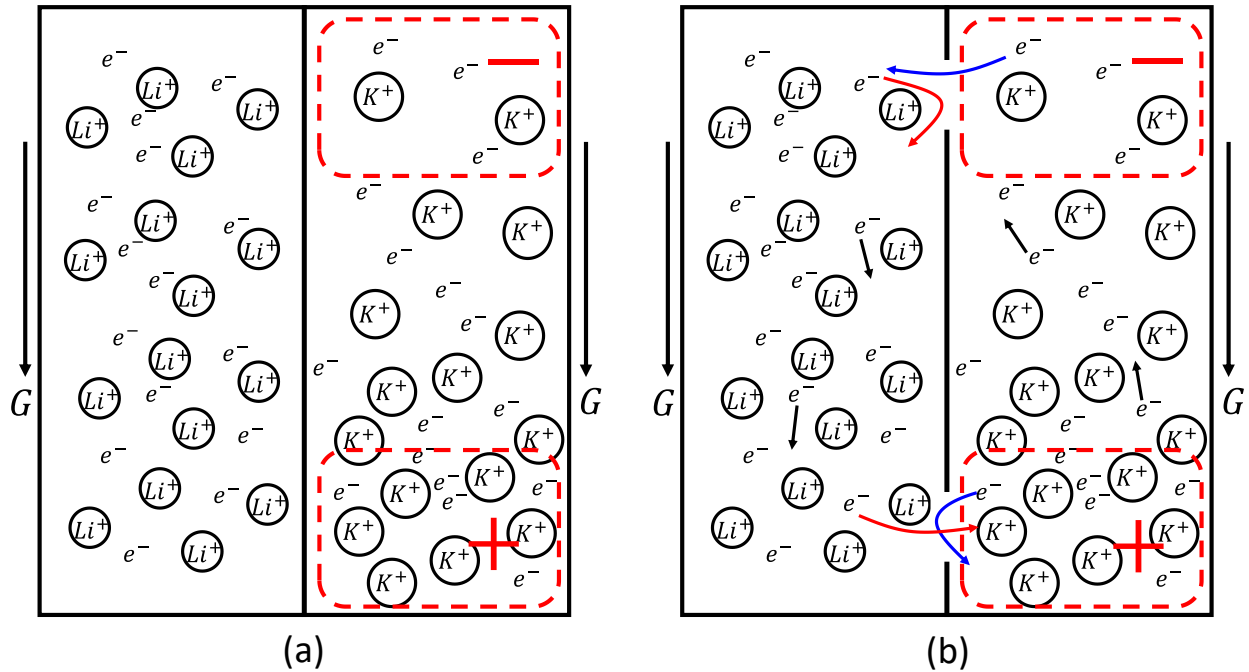


**Fig. 2.** Illustrates the concept via an approach similar to Maxwell's reasoning. (a) Two adjacent plasma bodies are shown, one being a potassium ion plasma and the other being a lithium ion plasma. Each plasma is treated as independent, with the potassium ion plasma exhibiting a more pronounced potential difference, showing negative bias at the upper region and positive bias at the lower region. In contrast, lithium-ion plasma has minimal and less noticeable potential deviation. (b) Small openings are introduced at both the upper and lower regions of the two plasma bodies. At the upper opening, the negatively biased potassium ion plasma repels electrons from the lithium ion plasma, causing these electrons to be more likely to move back toward the lithium ion plasma owing to the repulsive force. At lower openings, the positively biased potassium ion plasma has the opposite effect, attracting electrons from the lithium ion plasma.

Since the mass of electrons is significantly smaller than that of lithium ions, referencing Equation (3), the electric field strength within the lithium-ion plasma can be approximated by

Equation (5). Similarly, the electric field strength within the potassium-ion plasma can be approximated by Equation (6).

$$E_{in.Li^+.plasma} \cong -\frac{m_{Li^+}G}{2q} \dots \dots \dots (5)$$

$$E_{in.K^+.plasma} \cong -\frac{m_{K^+}G}{2q} \dots \dots \dots (6)$$

By comparing Equations (5) and (6), when the height difference between the upper and lower apertures is h, the subtracted value of the voltage difference between the two regions can be obtained as described in Equation (7).

$$\Delta(\Delta V) = E_{Li^+.plasma} \times h - E_{K^+.plasma} \times h = \frac{(m_{K^+} - m_{Li^+})Gh}{2q} > 0 \dots \dots \dots (7)$$

From Equation (7), the total energy released can be determined by summing the average electrical energy released when one additional electron flows from the potassium-ion plasma to the lithium-ion plasma through the upper aperture and the average electrical energy released when one additional electron flows from the lithium-ion plasma to the potassium-ion plasma through the lower aperture, as described in Equation (8).

$$q\Delta(\Delta V) \cong \frac{1}{2}(m_{K^+} - m_{Li^+})Gh > 0 \dots \dots \dots (8)$$

Equation (8) shows that, in a potassium-ion plasma, pushing an electron from a lower position to a higher position requires overcoming the gravitational attraction of potassium ions, consuming thermal vibrational energy approximately equal to half the product of the potassium ion mass, gravitational acceleration, and height difference. Conversely, in a lithium-ion plasma, when an electron moves downward from a higher position, it gains kinetic energy due to the gravitational attraction of lithium ions, and this energy is subsequently converted into thermal energy, with an average value approximately equal to half the product of the lithium-ion mass, gravitational

acceleration, and height difference. Since potassium ions are heavier than lithium ions are, the net thermal-to-electrical conversion energy in a circulating electron flow can be positive, meaning that the system releases a net positive thermal energy, thereby reducing entropy by an amount equal to half the product of the mass difference between potassium and lithium ions, gravitational acceleration, and height difference divided by the absolute temperature. This phenomenon surpasses the limitations of Carnot's theorem and represents an exception to the second law of thermodynamics.

## **5. Electric Field Formation and Voltage Difference Across Ionic Aqueous Solutions in a Gravity Field**

The previous paragraph used plasma as a theoretical deduction. However, ion plasma requires high temperatures and is difficult to control and operate; however, at normal temperatures, ions can be found in aqueous solutions. Considering an ionic aqueous solution, when the net masses or mass–charge ratios of positive and negative ions in water (the weight of the ions minus the buoyancy force of the water on the ions) are different, a potential difference can also be generated by gravity. As demonstrated in Tolman's 1910 experiment, the offset voltage of a lithium iodide aqueous solution under a specific rotational speed (approximately 70 units) was approximately  $4.3 \text{ mV}^3$ , whereas the offset voltage of a potassium iodide aqueous solution under the same rotational speed (and thus the same centrifugal force) was approximately  $3.5 \text{ mV}^3$ , indicating a significant difference.

If a setup similar to that in Fig. 2 is used, with one side replaced by a lithium iodide aqueous solution instead of lithium plasma and the other side replaced by a potassium iodide aqueous solution instead of potassium plasma, the openings at the top and bottom should be replaced with electrode plates that can exchange electrons between the two container spaces

without exchanging ions and replace the openings at the top and bottom with electrode plates that can exchange electrons between the two container spaces without exchanging ions. Similar voltage differences and thermoelectric conversion effects can be achieved.

Next, we employ a configuration in which one side is an aqueous electrolyte solution and the other side is a copper conductive plate as the basis for calculations and experiments. As Tolman mentioned in his 1916 paper, the offset voltage in metals under the same acceleration is significantly smaller than that in ionic liquids <sup>6</sup>, suggesting that a similar effect should also be achievable.

### *5.1 Estimation of Output Energy In the Case where the pH of the Ionic Aqueous Solution Deviates Significantly from 7*

In cases where the pH value deviates significantly from 7, the primary ions in an acidic ionic solution are solute anions and hydrogen ions, whereas the primary ions in a basic ionic solution are solute cations and hydroxide ions. When considering the built-in electric field within an accelerating force field, only these major ions need to be accounted for.

To estimate the potential energy output, we consider an aqueous solution of hydrogen iodide. In Figure 3, the gray region represents a high-strength aluminum alloy, which is assumed to have a yield strength of  $Y=670$  MPa. The blue region represents the electrolyte solution, which consists of hydrogen iodide in water. The distance from the center of the large circular disk to the center of the cross-section of the annular electrolyte is denoted as  $r_3$ . The cross-sectional radius of the electrolyte solution is  $r_1$ , whereas the outer radius of the cross-sectional hollow annular structure containing the electrolyte is  $r_2$ . The aluminum alloy disk has a thickness  $d$  of approximately  $r_3 - r_2$  from the disk center.

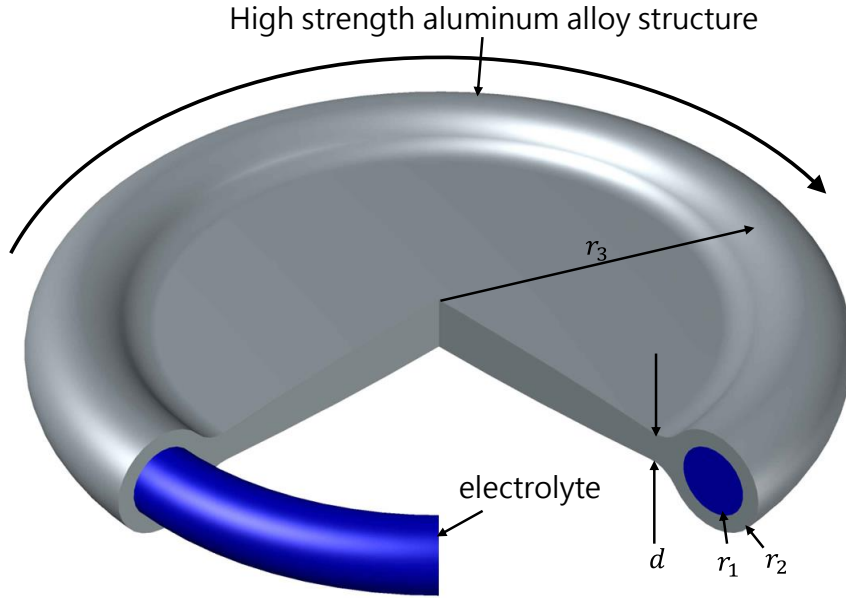


**Fig. 3.** Illustrates the structural configuration and dimensional notations used for simulating the maximum electrical power output

At a rotational speed  $\omega$ , the centrifugal force per unit volume of the electrolyte is approximately  $\rho_{liquid} \times r_3 \times \omega^2$ , where  $\rho_{liquid}$  is the density of the electrolyte solution. Consequently, the centrifugal force on the electrolyte per unit length along the radius  $r_3$  is  $\pi \times r_1^2 \times \rho_{liquid} \times r_3 \times \omega^2$ . The hollow annular aluminum alloy structure along the radius  $r_3$  experiences a centrifugal force per unit length of  $\pi \times (r_2^2 - r_1^2) \times \rho_{solid} \times r_3 \times \omega^2$ , where  $\rho_{solid}$  is the density of the high-strength aluminum alloy. Assuming that the centrifugal force is fully supported by the tensile strength of the annular structure along  $r_3$ , the maximum tolerable rotational speed  $\omega_1$  can be derived, resulting in Equation (9).

$$\pi(r_2^2 - r_1^2)Y = (\pi\rho_{solid}(r_2^2 - r_1^2)r_3\omega_1^2 + \pi\rho_{liquid}r_1^2r_3\omega_1^2)r_3$$

$$\Rightarrow \omega_1^2 = \frac{(r_2^2 - r_1^2)Y}{r_3^2(\rho_{solid}(r_2^2 - r_1^2) + \rho_{liquid}r_1^2)} \dots \dots \dots (9)$$

Alternatively, assuming that the centrifugal force is entirely supported by the inward tensile force of the disk, the maximum tolerable rotational speed  $\omega_2$  directed toward the center can be derived, resulting in Equation (10).

$$Yd \frac{r_3 - r_1}{r_3} = \pi \rho_{solid} (r_2^2 - r_1^2) r_3 \omega_2^2 + \pi \rho_{liquid} r_1^2 r_3 \omega_2^2$$

$$\Rightarrow \omega_2^2 = \frac{Y(r_3 - r_1)d}{\pi r_3^2 (\rho_{solid} (r_2^2 - r_1^2) + \rho_{liquid} r_1^2)} \quad \dots \dots \dots (10)$$

When both the tensile force in the annular structure and the inward tensile force act simultaneously, the maximum tolerable rotational speed  $\omega_3$  can be derived by combining Equations (9) and (10), resulting in Equation (11).

$$\omega_3^2 = \omega_1^2 + \omega_2^2 = \frac{[(r_2^2 - r_1^2) + (r_3 - r_1)d]Y}{r_3^2 (\rho_{solid} (r_2^2 - r_1^2) + \rho_{liquid} r_1^2)} \quad \dots \dots \dots (11)$$

By selecting parameters  $r_1 = 0.0025$  m,  $r_2 = 0.00355$  m,  $r_3 = 0.005$  m,  $d = 0.0021$  m,  $\rho_{solid} = 2700$  kg/m<sup>3</sup>, and  $\rho_{liquid} = 1000$  kg/m<sup>3</sup>, substitution into Equation (12) yields  $\omega_3^2 = 9.1888 \times 10^9$  sec<sup>-2</sup>. The maximum acceleration experienced by the electrolyte solution can then be calculated as  $\omega_3^2 r_3 \cong 4.5944 \times 10^7$  m/sec<sup>2</sup>. In solution, both the iodide anions and hydrogen cations are subjected to the same acceleration. Owing to the large mass of iodide ions, the buoyant force in water is negligible. Similarly, the buoyant force on hydrogen ions, with their small volume, can also be neglected. Using the approximate calculation method from Equation (4), the resulting electric field is estimated to be 29.97 V/m. Here, the mass of the iodide ion is approximately  $2.1073 \times 10^{-25}$  kg<sup>7</sup>, the mass of the hydrogen ion is  $1.1526 \times 10^{-26}$  kg<sup>7</sup>, and the elementary charge is  $-1.602 \times 10^{-19}$  C. The conductivity of the hydrogen iodide solution can be adjusted to 0.85 S/m<sup>14</sup>, resulting in a resistance of approximately 1.1765  $\Omega$  for a 1 m<sup>3</sup> cube. Assuming that the maximum output voltage drop is half the maximum voltage, the energy

output of the cube can be estimated as  $(29.97/2)^2/1.1765$  W. In addition to the effects of the annular structure, the energy output per unit volume of  $1 \text{ m}^3$  is approximately 72 W. This energy density falls within an acceptable range for power generation applications. Some other conditions are listed in Table 1.

Parameter	$r_1 = 0.0025 \text{ m}$	$r_1 = 0.01 \text{ m}$	$r_1 = 0.04 \text{ m}$
$r_2 \text{ (m)}$	0.00355	0.0142	0.0568
$r_3 \text{ (m)}$	0.005	0.02	0.08
$d \text{ (m)}$	0.0021	0.0084	0.0336
$\rho_{solid} \text{ (kg/m}^3\text{)}$	2700	2700	2700
$\rho_{liquid} \text{ (kg/m}^3\text{)}$	1000	1000	1000
$m_{H^+} \text{ (kg)}^{12,13}$	$1.1526 \times 10^{-26}$	$1.1526 \times 10^{-26}$	$1.1526 \times 10^{-26}$
$m_{I^-} \text{ (kg)}^{12,13}$	$2.1073 \times 10^{-25}$	$2.1073 \times 10^{-25}$	$2.1073 \times 10^{-25}$
Y (MPa)	670	670	670
$\omega_1^2 \text{ (sec}^{-2}\text{)}$	$7.275 \times 10^9$	$4.547 \times 10^8$	$2.842 \times 10^7$
$\omega_2^2 \text{ (sec}^{-2}\text{)}$	$1.914 \times 10^9$	$1.196 \times 10^8$	$7.476 \times 10^6$
$\omega_3^2 \text{ (sec}^{-2}\text{)}$	$9.189 \times 10^9$	$5.743 \times 10^8$	$3.589 \times 10^7$
$a \text{ (m/sec}^{-2}\text{)}$	$4.594 \times 10^7$	$1.1486 \times 10^7$	$2.872 \times 10^6$
E (V/m)	29.97	7.494	1.8734
Conductivity (S/m)	0.85	0.85	0.85
$P_{liquid}/\text{m}^3 \text{ (W/m}^3\text{)}$	190.92	11.933	0.7458
$P_{solid+liquid}/\text{m}^3 \text{ (W/m}^3\text{)}$	72.23	4.514	0.2821

**Table 1.** The simulation results for the output power of a hydrogen iodide solution were calculated for selected cross-sectional radii of the electrolyte ring at 0.0025 m, 0.01 m, and 0.04 m.

## 5.2 Conducting experiments in ionic aqueous solutions with a pH value close to 7

From the previous derivations and calculations, it is evident that achieving significant voltage changes requires extremely strong centrifugal forces, making experimental

measurements challenging. However, chemical titration experiments have demonstrated that in strong-electrolyte aqueous solutions, when the pH is close to 7, even slight variations in the ion concentration can result in significant pH changes. These pH changes can be measured as potential differences via a pH meter. Therefore, when the pH is close to 7, it becomes easier to measure the voltage difference caused by gravity.

Practically, this principle can be leveraged to amplify voltage differences and increase energy output, although further experiments are necessary to verify the specific conditions and effects. When the pH is close to 7, small changes in the ion concentration can lead to significant variations in the potential. Conversely, when the pH deviates significantly from neutrality—becoming either higher or lower—the same changes in ion concentration result in much smaller potential variations. This phenomenon indicates that the relationship between the voltage change and the centrifugal force exhibits nonlinear characteristics when the pH approaches neutrality (approximately 7).

To facilitate observation and measurement, we selected a potassium chloride aqueous solution as the experimental medium for this study. Because chloride ions and potassium ions are both strong electrolytes, they are almost completely dissociated. Owing to the effect of gravity, the potential energy of the ions changes, causing the ion concentration to change with height. The concentrations of chloride ions and potassium ions change with height due to the potential energy difference caused by gravity. According to Boltzmann's distribution law,<sup>5</sup> the concentration changes with height in the steady state without convection can be obtained as shown in equations (12) and (13):

$$[C_{K^+}]_h = [C_{K^+}]_0 e^{-\frac{m_{K^+} \cdot net \cdot Gh}{kT}} \quad \dots \dots \dots \quad (12)$$

$$[C_{Cl^-}]_h = [C_{Cl^-}]_0 e^{-\frac{m_{Cl^-} \cdot net \cdot Gh}{kT}} \quad \dots \dots \dots \quad (13)$$

where  $h$  is the height coordinate value,  $[C_{K^+}]_h$  is the potassium ion concentration at height  $h$ ,  $[C_{K^+}]_0$  is the potassium ion concentration at height 0,  $m_{K^+.net}$  is the net effective mass of potassium ions after accounting for buoyant force in water,  $[C_{Cl^-}]_h$  is the chloride ion concentration at height  $h$ ,  $[C_{Cl^-}]_0$  is the chloride ion concentration at height 0, and  $m_{Cl^-.net}$  is the net effective mass of chloride ions after accounting for buoyant force in water.

When calculating the net mass of an ion, the buoyant force exerted by water on the ion must be subtracted from the mass of the ion, as the densities of potassium ions and chloride ions are relatively close to those of water molecules, making the buoyant force significant and unable to be ignored. To determine this buoyant force, the effective volume of the ion is first calculated. This volume is then multiplied by the density of water to obtain the buoyant force acting on the ion. A KCl aqueous solution with a concentration of 2 N was used as an example.

On the basis of the density of HCl at a concentration of 2 N ( $1.03008 \text{ g/cm}^3$ )<sup>8</sup> and at a concentration of 1.8 N ( $1.02690 \text{ g/cm}^3$ )<sup>8</sup> and considering that the volume of hydrogen ions is negligible, the effective volume of chloride ions at a concentration close to 2 N is estimated to be approximately  $3.2928 \times 10^{-23} \text{ cm}^3$ . The net mass of chloride ions, after the buoyant force of water at this concentration is subtracted, is calculated to be approximately  $2.3252 \times 10^{-26} \text{ kg}$ .

Similarly, on the basis of the density of KCl at a concentration of 2 N ( $1.08166 \text{ g/cm}^3$ )<sup>9</sup> and at a concentration of 1.8 N ( $1.07390 \text{ g/cm}^3$ )<sup>9</sup> and the previously determined effective volume of chloride ions, the effective volume of potassium ions at a concentration close to 2 N was estimated to be approximately  $1.8608 \times 10^{-23} \text{ cm}^3$ . The net mass of potassium ions, after the buoyant force of water at this concentration is subtracted, is calculated to be approximately  $4.4797 \times 10^{-26} \text{ kg}$ .

Substituting the net masses of chloride and potassium ions into Equations (12) and (13), the variation in the chloride and potassium ion concentrations with height under an acceleration equivalent to Earth's gravitational acceleration (assuming equal concentrations of chloride and potassium ions at the reference height) is shown in Figure 4.

Since both potassium and chloride ions are strong electrolytes, they dissociate nearly completely in water. When chloride ions are more abundant than potassium ions are, the hydrogen ions that dissociate from water compensate to achieve electrical neutrality. Conversely, when chloride ions are less abundant than potassium ions are, hydroxide ions that dissociate from water compensate for the electrical balance. Using the fundamental laws of pH, the variation in pH with height can be determined and is shown in Figure 5.

By applying the Nernst equation (Equation (14))<sup>10</sup>, the voltage variation with height can be calculated. When the electrode primarily exchanges electrons with chloride ions, the voltage variation is represented by the solid line in Figure 6. When the electrode primarily exchanges electrons with potassium ions, the voltage variation is represented by the dashed line in Figure 6. If the electrode primarily exchanges electrons with hydrogen ions or hydroxide ions, the voltage variation with height is shown as the solid line in Figure 7.

$$\Delta V = -\frac{RT}{nF} \ln \left( \frac{[C]}{[C]_0} \right) \quad \dots \dots \dots \quad (14)$$

Figure 7 also reveals that when the electrode exchanges electrons primarily with hydrogen ions or hydroxide ions, the voltage variation with height is nonlinear. This nonlinear behavior can explain the phenomena observed in our experiments.

changes in chloride ion concentration and potassium ion concentration with height under the steady state without convection

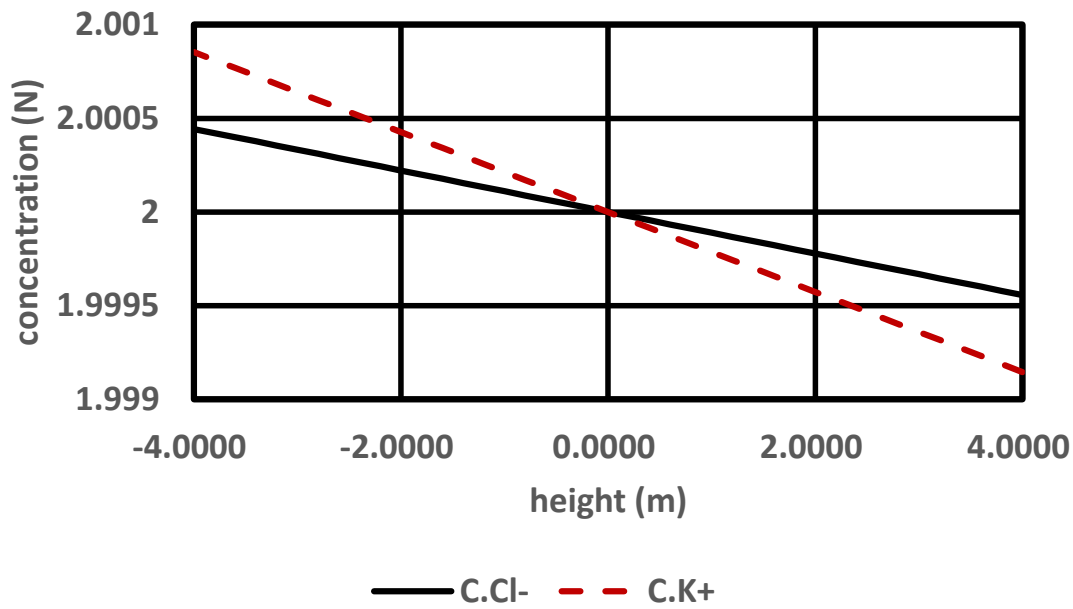


**Fig. 4.** The concentrations of chloride ions and potassium ions at zero height are both 2 N, and the changes in the chloride ion concentration and potassium ion concentration with height are under the steady state without convection. The vertical axis is the concentration value in N, and the horizontal axis is the height value in m.

changes in pH value with height under the steady state without convection

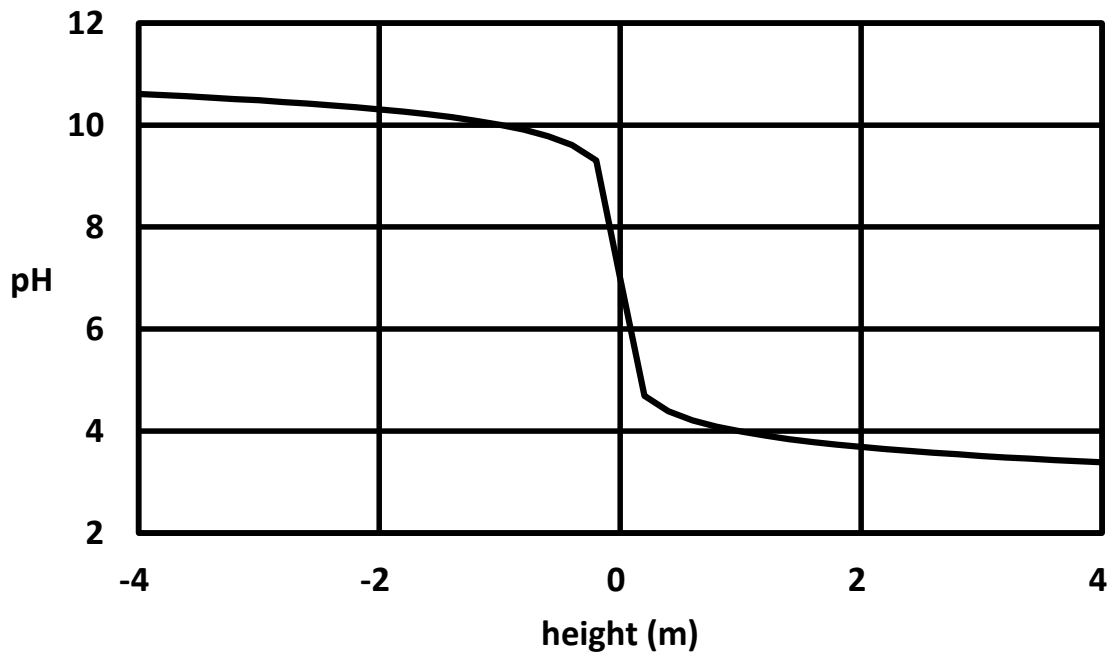


**Fig. 5.** The calculated pH value of the KCl aqueous solution at equilibrium. The vertical axis represents the pH value, and the horizontal axis represents the height in m.

Potential changes with height when the electrode exchanges electrons with chloride ions and exchanges electrons with potassium ions

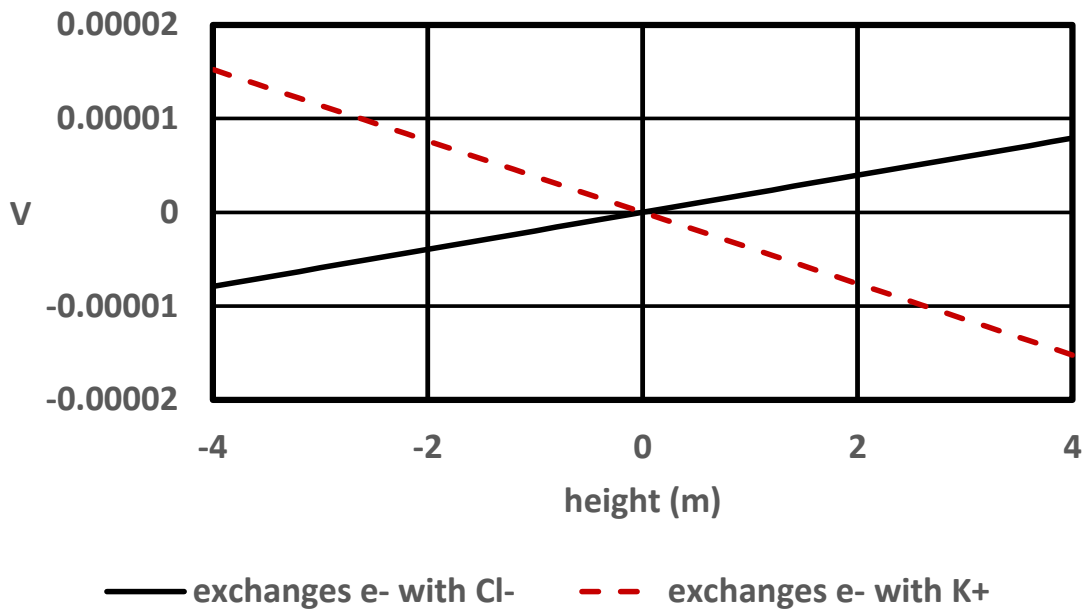


**Fig. 6.** The potential changes with height when the electrode exchanges electrons with chloride ions and exchanges electrons with potassium ions.

### The change in potential with height when the electrode exchanges electrons with hydrogen ions or hydroxide ions

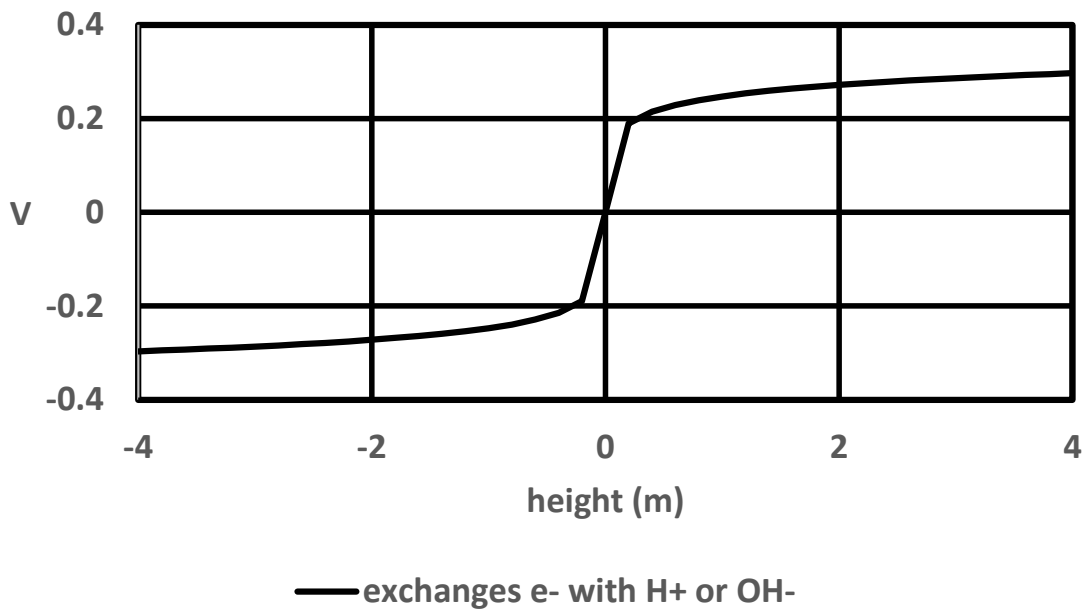


**Fig. 7.** The change in potential with height when the electrode exchanges electrons with hydrogen ions or hydroxide ions.

The lower the pH is, the higher the concentration of hydrogen ions, and the opposite is true for hydroxide ions. Fig. 5 shows that the concentration of hydrogen ions is greater at high positions, and the concentration of hydroxide ions is greater at low positions. When the upper and lower ends are connected to a resistor, the resistor links the two ends, altering the voltage and causing the ion concentrations to deviate from equilibrium, thus initiating diffusion. In this process, the hydrogen ions above diffuse downward, whereas the hydroxide ions diffuse upward, meeting and combining in the central area to form water. This is similar to what occurs in plasma, where the diffusion energy of atoms and ions is also derived from the thermal energy of thermal vibrations. The downward movement of positively charged hydrogen ions and the

upward movement of negatively charged hydroxide ions can both create internal currents from top to bottom, thus forming a gravity battery that outputs electrical energy through an external resistor. Similarly, when positively charged potassium ions and negatively charged chloride ions diffuse upward or downward, an electric current is also generated. Therefore, the energy is sent out without a temperature difference.

The above discussion theoretically examines the changes in concentration and electric field within plasma or ionic solutions under the influence of gravitational or centrifugal forces, essentially in the presence of acceleration. The following section describes our experimental approach to validate this phenomenon and how we measured continuous and stable current outputs in the absence of a temperature difference.

## **6. Experimental Verification**

Tolman's experimental data from 1910 are almost sufficient as the basis for our inference. The only remaining question to verify is whether, as Tolman suggested, the polarization effect causes the voltage and current to gradually approach zero as the charge accumulates or if, as we hypothesize, the voltage and current can remain stable and continuously output electrical energy over an extended period without gradual decay.

To verify our hypothesis, we designed a structure resembling a battery in which positive and negative ions with different masses experience different forces in a centrifugal or gravitational field. This results in a potential difference at the terminals, and we measured whether this potential difference could provide a stable and long-term energy output. The fabrication and testing of the gravity battery involved several key steps, with each main experimental stage detailing the materials and equipment used, along with the rationale behind their selection.

### 6.1. Materials, Methods, & Procedures

1. *Electrode Preparation:* A titanium electrode plate (1 mm thick, 99.5% pure) was selected for its stability and was coated with a 1  $\mu\text{m}$  thick layer of platinum on both sides through electroplating. This platinum coating not only minimizes potential differences but also renders the electrode inert, significantly reducing the likelihood of chemical reactions with the electrolyte in the gravity battery. The platinum-coated titanium sheet was then cut into circular electrodes with a diameter of 50 mm via a water jet to ensure low temperatures during the cutting process, thereby preserving the physical and chemical properties of the electrode surface.
2. *Cavity Formation:* Multiple silicone sheets, each with an outer diameter of 60 mm and an inner diameter of 40 mm, were used to form cavities for the gravity battery units. Silicone was chosen as the cavity material because of its chemical inertness, which prevents any reaction with ions in the electrolyte.
3. *Electrolyte Solution:* A potassium chloride solution (99.9% pure) was prepared with the pH adjusted to near neutrality ( $\text{pH} \approx 7$ ) to serve as the electrolyte. Potassium chloride was selected because the net weights of chloride and potassium ions in water, after accounting for buoyancy, significantly differ, enhancing the system's response. The theoretical derivation suggested that the largest voltage change occurs when the pH is close to 7. Therefore, a 2 N KCl aqueous solution with a pH near 7 was prepared through vacuum degassing, which minimizes gas bubbles that could otherwise obstruct potential conduction or current flow. However, vacuum degassing also poses the risk of altering the pH by removing trace amounts of chlorine gas. Two gravity cells with different

degassing durations were prepared. The longer degassing time of one cell led to a slight reduction in the chloride ion concentration due to chlorine gas removal.

4. *Battery Assembly:* The materials described above were used to assemble two gravity battery packs, each consisting of six small gravity cells electrically connected in series. The electrode spacings within the cells were set at 2 mm, 4 mm, 8 mm, 16 mm, 24 mm, and 32 mm. The arrangement is depicted in Figure 8. Arranging multiple cells with varying electrode spacings allows any significant reaction in one of the cells to be easily detected and measured, ensuring reliable data collection across different spacing conditions. Once prepared, the degassed KCl solution was injected into each cavity of the gravity cells, and the openings were sealed. The electrode connections were then completed, as shown in the center panel of Figure 9.
5. *External Connections and Housing:* Copper sheets (99% pure) were employed for external electrical connections because of their relatively low resistance, which helps minimize measurement deviations caused by external resistance and improves overall measurement accuracy. The assembled gravity battery was housed in a 304 stainless steel casing and sealed with epoxy resin to ensure stability during testing. Stainless steel was chosen for its high strength and chemical inertness, preventing deformation under high gravity or centrifugal forces and ensuring that it would not corrode or degrade over prolonged measurements.
6. *Centrifuge Testing Setup:* The battery pack was placed in a centrifuge with a rotation radius of 1200 mm and balanced by placing them opposite one another to maintain a stable center of gravity. The centrifuge was accelerated to generate a

centrifugal force equivalent to 10 times the gravitational force at the Earth's surface (10G). The large rotation radius was selected to ensure that the direction of the centrifugal force remained precisely vertical across different parts of the electrodes, whereas high acceleration was chosen to amplify the voltage, making it easier to measure.

7. *Voltage Measurement During Centrifugation:* The centrifuge was operated at 10 G (ten times Earth's gravity) for two hours, during which the voltage output was continuously monitored. This duration allowed sufficient diffusion time for the solution to reach a near-equilibrium ion concentration gradient, confirming that a voltage difference can be generated under high centrifugal force. Voltage and time data were recorded via an MMV-387SD three-channel voltage data recorder (Lutron, Sunwe Co., Taiwan) with a resolution of 0.1 mV. After the centrifugal force measurements, the cells were allowed to rest for 30 minutes, during which the discharge process was recorded, demonstrating that the voltage difference disappears once the centrifugal force is removed.
8. *Long-term Stability Test:* To fully discharge the gravity cells and remove any residual charge, they were short-circuited and left horizontally for 290 days (with gravity parallel to the electrode plates). The samples were subsequently placed vertically (gravity perpendicular to the electrode plates) for three days to allow the ion distribution to stabilize under gravity, as shown in the left panel of Figure 10. The gravity battery was then oriented in a forward position, ensuring that the electrode surfaces were perpendicular to the direction of gravity. To determine whether a continuous current output could be sustained over time, a 6.8 M $\Omega$  resistor was connected across the electrodes of the vertically placed gravity cell,

and the system was monitored over a period of 55 days. This setup aimed to verify that the generated voltage could persist over an extended duration with power output, confirming that it was not merely a transient phenomenon. The entire experiment was conducted in a room with a day–night temperature variation of less than 1.5°C, and the sample was placed in an iron cabinet to ensure no electromagnetic interference and no uneven temperatures caused by air convection." Voltage measurements were taken via a Keysight 34465A digital multimeter (Keysight Technologies, Santa Rosa, CA, United States) with a resolution of 0.1  $\mu\text{V}$ . As shown in Figure 10, the left image illustrates the system in its stationary state, whereas the right image depicts the system with a 6.8 M $\Omega$  resistor connected between the positive and negative electrodes. The voltage was measured six times between the 15th and 55th days.

9. *Inverted Position Test:* The gravity battery was then inverted (placed upside down) and subjected to a similar long-term test over 86 days, with voltage readings taken via the same Keysight multimeter setup. Voltage measurements were taken 24 times between the 33rd and 86th days. This was done to confirm that the voltage was indeed caused by gravitational acceleration, with the hypothesis that reversing the direction of gravity would result in an opposite voltage. Therefore, the sample was inverted for measurement.

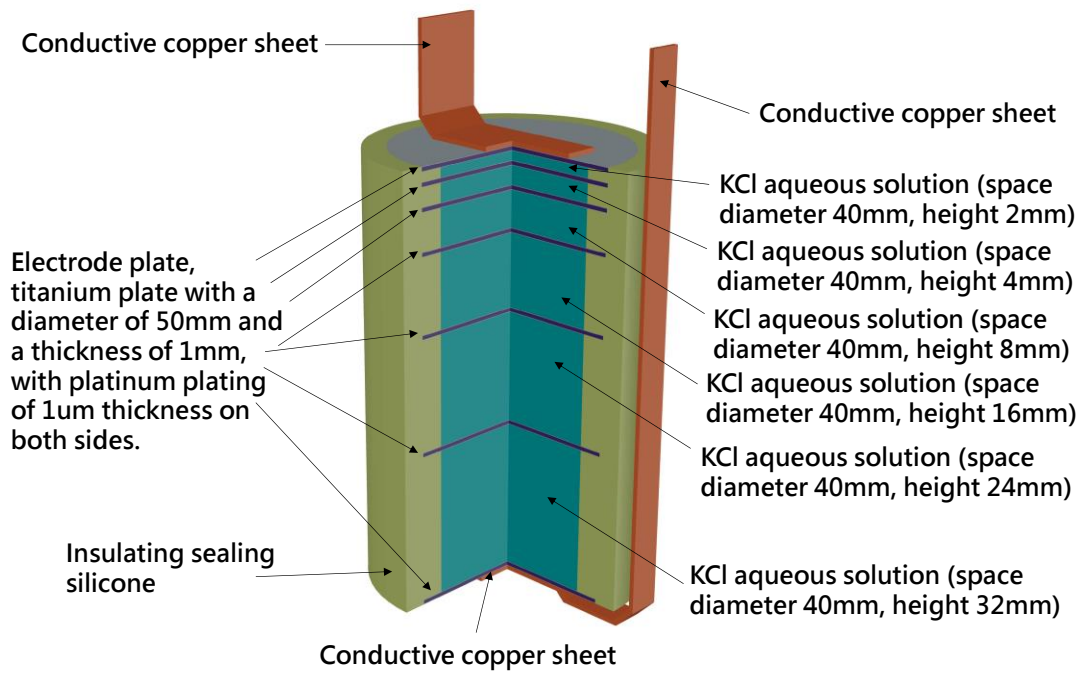


**Fig. 8.** Internal structure diagram of the gravity battery, including six small units with electrode spacings of 32 mm, 24 mm, 16 mm, 8 mm, 4 mm, and 2 mm that are electrically connected in series.



**Fig. 9.** Selected images of the gravity battery production process.



**Fig. 10.** Selected images of the gravity battery during the static measurement process.

### *6.2. Experimental Results*

The left panel of Figure 11 shows the experimental setup, whereas the right panel illustrates the relationship between the output voltage and time under a 10 G centrifugal force field. As the 10G field was applied, the voltage difference between the two gravity batteries gradually increased, confirming that the centrifugal force induced potential changes in the solution along the direction of the field. This suggests that the device can continuously convert ambient thermal energy into electrical energy when exposed to a sufficiently large gravitational or centrifugal force. Small differences in pH between the two gravity batteries led to variations in the timing and magnitude of the generated potentials. Once the centrifuge stopped and no centrifugal force was applied, the potential quickly returned to its initial state.

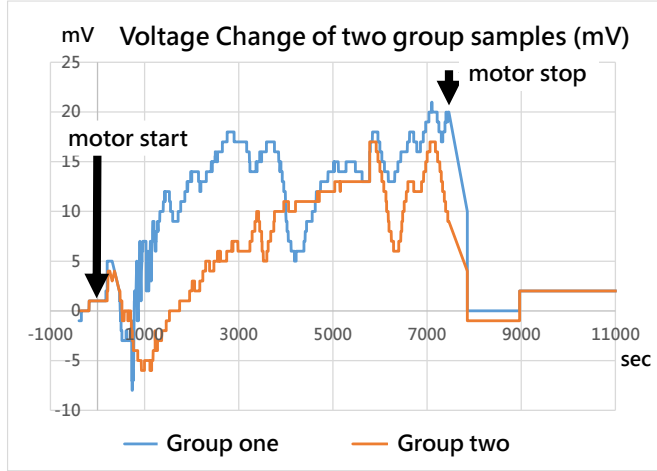
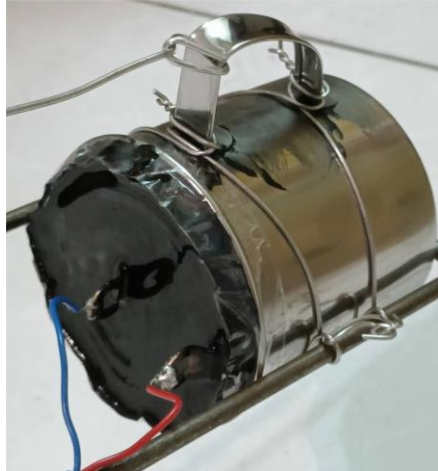


**Fig. 11.** The gravity battery unit was subjected to a centrifugal force field of 10 G (10 times the gravity of the Earth's surface), and the output voltage was continuously recorded for two hours. The resulting relationship between the measured potential and time is shown.

Table 2 summarizes the voltage measurements from the first and second samples when placed vertically with a 6.8 MΩ load from a resistor. The first sample exhibited an average output voltage of 22.594 mV with a standard deviation of 3.240 mV over 40 days (15<sup>th</sup> to 55<sup>th</sup>), whereas the second sample had an average output voltage of -0.647 mV with a standard deviation of 0.503 mV. Individual measurements for both samples are listed in the table.

Sample	Day 15	Day 25	Day 34	Day 41	Day 48	Day 55
1st	26.460 mV	25.571 mV	22.611 mV	19.423 mV	23.181 mV	23.181 mV
2nd	-0.331 mV	-0.123 mV	-0.272 mV	0.750 mV	-0.959 mV	-0.959 mV
Sample	Mean	Standard Deviation				
1st	22.594 mV	3.240 mV				
2nd	-0.647 mV	0.503 mV				

**Table 2.** Voltage measurements from the first and second samples when placed vertically with a 6.8 MΩ load from a resistor.

To confirm that the potential difference is due to gravity, the opposite voltage should be measured when the gravity cell is turned upside down. When the same samples were placed upside down, the voltage began to change. The average output voltage of the first sample from the 33rd day to the 86th day was -4.169 mV, and the measurement standard deviation was 1.396 mV; the average output of the second sample was 11.148 mV, and the measurement standard deviation was 0.282 mV.

Table 3 summarizes the voltage measurements from the first and second samples when placed upside down with a 6.8 MΩ load from a resistor.

Sample	Day 33	Day 35	Day 37	Day 39	Day 41	Day 44
1st	-2.113 mV	-1.149 mV	-1.895 mV	-2.476 mV	-2.028 mV	-2.928 mV
2nd	11.702 mV	11.496 mV	11.241 mV	11.189 mV	10.871 mV	10.938 mV
Sample	Day 46	Day 48	Day 51	Day 53	Day 55	Day 58
1st	-5.729 mV	-6.162 mV	-5.669 mV	-4.141 mV	-3.860 mV	-4.732 mV
2nd	11.311 mV	10.733 mV	11.718 mV	11.302 mV	11.345 mV	11.244 mV
Sample	Day 60	Day 62	Day 65	Day 67	Day 69	Day 72
1st	-4.320 mV	-5.309 mV	-4.546 mV	-4.727 mV	-4.489 mV	-4.878 mV
2nd	11.362 mV	11.167 mV	10.909 mV	11.049 mV	11.215 mV	11.040 mV
Sample	Day 74	Day 76	Day 79	Day 81	Day 83	Day 86
1st	-4.066 mV	-4.959 mV	-4.295 mV	-6.263 mV	-5.091 mV	-4.234 mV
2nd	11.193 mV	11.204 mV	10.901 mV	11.064 mV	10.771 mV	10.577 mV
Sample	Mean	Standard Deviation				
1st	-4.169 mV	1.396 mV				
2nd	11.148 mV	0.282 mV				

**Table 3.** Voltage measurements from the first and second samples when placed upside down with a 6.8 MΩ load from a resistor.

## 7. Discussion

The measurement results show that the output voltages of the upright and upside-down devices are opposite. Moreover, the voltage directions of the two samples are different when they are standing. According to our previous theoretical calculations, when the electrode exchanges electrons with different ions or when the pH is different, the voltage difference will be different and may be opposite.

In centrifugal force experiments, a voltage bias is generated because of the presence of a centrifugal force and disappears when the centrifugal force is removed, leading to the conclusion that the centrifugal force is responsible for the potential difference. In experiments directly utilizing Earth's gravity, stable current and electrical energy output were maintained regardless of whether the system was placed upright or inverted, indicating that this voltage difference is not limited to a temporary state but represents a stable, steady condition. These experiments demonstrate that continuous energy conversion occurs in both gravitational and centrifugal force fields. According to the law of conservation of energy and supported by earlier theoretical derivations, the energy source is identified as the thermal energy from the environment. Our measurements are consistent with the phenomenon observed by T. Dale Stewart and Richard C. Tolman in 1910.<sup>3</sup>

When a force acts on the same physical properties of ions, since the ions move in a random and scattered manner, it must comply with Carnot's theorem,<sup>1</sup> which states that the maximum energy output rate of a heat engine cannot be greater than the temperature difference divided by the absolute temperature. However, when an electric field affects the charge of an ion, gravity affects the mass of the ion. The forces experienced by ions with different masses are unequal, imparting directional characteristics to ion motion. This article raises the question of whether, in cases where ions of different masses exhibit diverse directional tendencies, it might

be possible to surpass the constraints imposed by Carnot's theorem. <sup>1</sup> In our theoretical derivation, a potential difference caused by gravity is indeed derived. Therefore, it is possible to convert thermal energy into electrical energy without a temperature difference.

Although the initial theoretical derivations were based on plasma, practical experiments with ion plasma are challenging because ion plasma extraction is difficult to perform via centrifugation; therefore, we opted instead to conduct experiments using aqueous ion solutions with ions of different masses or mass-charge ratios. The first aqueous ion solution to be considered is sodium chloride, which is the easiest to obtain. Chloride ions and sodium ions have the same charge and opposite electrical properties, and the ion masses greatly differ, so they may be good experimental objects. However, when the buoyancy force on the effective volume in solution is considered, because the volume of chloride ions is much larger than that of sodium ions, after the buoyancy force is deducted, the net masses of the two ions will be very close, so observing the voltage difference due to gravity is difficult. Therefore, we changed the solution to a potassium chloride aqueous solution with similar original masses of positive and negative ions but a large difference in effective volume. As we calculated in the previous article, there is a large difference in the net masses of chloride ions and potassium ions. In the experiment, the potential difference was indeed measured when the sample was placed upright and upside down. That is, the same sample will have different potential differences in different directions of gravity. It can also be inferred that the voltage difference is caused by gravity.

In limited measurements, the voltage and current that can be measured are very small, but it can still be proven that thermal energy is converted into electrical energy without a temperature difference.

To amplify the energy output, either increasing the rotational speed or reducing the radius can be effective strategies. A faster rotating centrifuge can significantly increase the energy output.

Reducing the rotation radius also contributes to a higher energy output. Since air resistance is proportional to the square of the rotational speed, a smaller radius allows the same acceleration to be achieved at a slower rotational speed, which corresponds to lower air resistance. Additionally, for the same rotational speed, a smaller radius results in a greater centrifugal force. This means that reducing the radius can achieve comparable acceleration with lower frictional losses, providing an efficient way to increase the energy output.

In terms of energy conversion efficiency. Potassium chloride is not the most energy-efficient combination of ingredients, but many other chemical combinations could be tested.

## **8. Conclusion**

Energy conversion is crucial for the sustainable operation of our planet. While concentration cells have been extensively studied and applied, the potential difference caused by concentration gradients resulting from gravity or centrifugal force has not received sufficient attention. With the insight provided by Richard C. Tolman's 1910 observation of voltage bias in conductors within an accelerated force field, it becomes clear that such forces can indeed generate a potential difference<sup>4</sup>. Our theoretical calculations confirm that this potential difference occurs not only on the surface of the conductor but also within its interior, further indicating that thermal energy can be converted into electrical energy—via driving charged particles to move against the electric field—even in the absence of a temperature difference. This process exceeds the limitations imposed by Carnot's theorem. We demonstrated this experimentally by using a centrifugal force or artificial gravity to generate a potential difference. Furthermore, by utilizing

natural gravity, we achieve a continuous current output. The reversal of the output voltage when the device is inverted further verifies that gravity can indeed produce a voltage difference and current. Moreover, since this electrical power output remained stable for over three months without any noticeable degradation—approximately 100 times longer than the time required for ions to diffuse about 20 mm in aqueous solution—it demonstrates that this is a sustained phenomenon rather than a transient polarization effect.

This study concludes that, in the absence of a temperature gradient, the use of gravity or a centrifugal force provides a feasible method for converting thermal energy into electrical energy, thereby overcoming the limitations imposed by Carnot's theorem. Although the mechanism for counteracting changes in ion concentration still requires further study, this approach holds promise as a viable green energy source. This discovery opens new avenues for research and practical applications in various directions.

## **ACKNOWLEDGMENTS**

We would like to acknowledge the professional manuscript services of American Journal Experts. Additionally, we extend our sincere gratitude to Wolfgang Sturm for providing valuable insights into the 'Stewart–Tolman effect', which greatly facilitated access to prior experimental results.

## **DATA AVAILABILITY STATEMENT**

Not applicable

## **DECLARATIONS**

**Conflict of interest statement**

The author has no conflicts of interest to disclose.

**Author Contributions**

Kuo Tso Chen designed the study, performed the experiments, analyzed the data, and wrote the manuscript.

**Ethics Approval**

I confirm that the manuscript has been approved by the author for publication. I declare that the work described herein is original research and that it has not been published previously.

## REFERENCES

- <sup>1</sup>Y. Izumida, "Irreversible efficiency and Carnot theorem for heat engines operating with multiple heat baths in linear response regime," *Phys. Rev. Res.* 4, 023217 (2022).
- <sup>2</sup>Milivoje M. Kostic, "The Second Law and Entropy Misconceptions Demystified", *Entropy* 2020, 22(6), 648 (2020), <https://www.mdpi.com/1099-4300/22/6/648> , Accessed 13 November 2024.
- <sup>3</sup>R.C. Tolman, "The Electromotive Force Produced in Solutions by Centrifugal Action", *Proc. Am. Acad. Arts Sci.* 46, 109 (1910),
- <sup>4</sup>Leff, H.S.; Rex, A.F. *Maxwell's Demon 2: Entropy, Classical and Quantum Information, Computing*; CRC Press: Boca Raton, FL, USA, 2002; ISBN 0-7503-0759-5.
- <sup>5</sup>BOLTZMANN, Ludwig, 'Studien über das Gleichgewicht der lebendigen Kraft zwischen bewegten materiellen Punkten.' *Sitzungsberichte der kaiserlichen Akademie der Wissenschaften*, LVIII. Band, Jahrgang 1868.
- <sup>6</sup>R. C. Tolman, and T. D. Stewart, "The electromotive force produced by the acceleration of metals," *Phys. Rev.* 8, 97–116 (1916).
- <sup>7</sup>T. Prohaska, J. Irrgeher, J. Benefield, J. K. Böhlke, L. A. Chesson, T. B. Coplen, T. Ding, P. J. H. Dunn, M. Gröning, N. E. Holden, H. A. J. Meijer, H. Moossen, A. Possolo, Y. Takahashi, J. Vogl, T. Walczyk, J. Wang, M. E. Wieser, S. Yoneda, X.-K. Zhu, and J. Meija, "Standard atomic weights of the elements 2021 (IUPAC Technical Report)," *Pure Appl. Chem.* 94, 573–600 (2022).
- <sup>8</sup>D. Rowland, "Density of hydrochloric acid, HCl(aq), advanced thermodynamics," *Advanced Thermodynamics*, 2021, Accessed 8 June 2023, [https://advancedthermo.com/electrolytes/density\\_HCl.html](https://advancedthermo.com/electrolytes/density_HCl.html).
- <sup>9</sup>D. Rowland, "Density of potassium chloride, KCl(aq), advanced thermodynamics," *Advanced Thermodynamics*, 2021, Accessed 8 June 2023, [https://advancedthermo.com/electrolytes/density\\_KCl.html](https://advancedthermo.com/electrolytes/density_KCl.html).
- <sup>10</sup>D. Larsen, "20.6: The Nernst equation1. Chemistry libretxts," (2016), Accessed 7 November 2023, [https://chem.libretxts.org/Courses/Heartland\\_Community\\_College/HCC%3A\\_Chem\\_162/20%3A\\_Electrochemistry/20.6%3A\\_The\\_Nernst\\_Equation](https://chem.libretxts.org/Courses/Heartland_Community_College/HCC%3A_Chem_162/20%3A_Electrochemistry/20.6%3A_The_Nernst_Equation).